QSAR & Combinatorial Science QCS

Prediction of Melting Points for Ionic Liquids

Steven Trohalaki and Ruth Pachter**

Air Force Research Laboratory, Materials & Manufacturing Directorate, 3005 Hobson Way, Suite 1, Wright-Patterson Air Force Base, OH 45433-7702, USA

Keywords: Ionic liquids, Melting Point Prediction, QSPR, Quantitative Structure-Property Relationships

Received on: November 9, 2004; Accepted on December 16, 2004

Abstract

Melting points are important for the specific application of ionic liquids. Although many different ionic liquids are possible, melting points are known only for relatively few. Derivation of melting point QSPRs (Quantitative Structure-Property Relationships) for ionic liquids would therefore greatly aid in the molecular design of new compounds. A new class of ionic liquids, based on 1-substituted-4-amino-1,2,4-triazolium bromide, nitrate, and nitrocyanamide salts were recently synthesized and their melting points measured. After optimizing the molecular geometries of the cations of the ionic liquids using ab initio quantum chemical methods, we derived melting-point QSPRs from molecular orbital and electrostatic descriptors. Good correlations with the experimental data were found. The correlation coefficients for three-parameter melting-point QSPRs exceed 0.8. Although some of the descriptors that appear in our QSPRs were designed to describe chemical reactions, we infer that they serve in this study to quantify interactions between the cation and anion or between the cations.

1 Introduction

Several hydrazine derivatives occur naturally in tobacco and mushrooms. Some hydrazines have been shown to be pharmacologically active and others are herbicides. Aerospace fuels contain hydrazine and its methyl derivatives because they are powerful reducing agents [1]. The introduction of hydrazine, monomethyl hydrazine, and 1,1-dimethyl hydrazine as aerospace fuels grew out of a need for high-energy, noncryogenic, liquid fuels that can be used alone or mixed with other components. The toxicity of hydrazine fuels is a substantial operational concern to the U.S. Department of Defense as well as to the aerospace industry. Inhalation and skin exposure are the two most likely occupational exposure routes [2]. We have previously reported quantitative structure-activity relationships for toxicity prediction of a series of high-energy compounds [3].

Ionic liquids have melting points that fall below room temperature. They have generated considerable interest as 'green' alternatives in current industrial applications because of their exceptional solvating ability and extremely low vapor pressures [4, 5, 6, 7, 8]. Because the exposure routes are greatly diminished due to their low vapor pressures, energetic ionic liquids should be inherently less toxic than hydrazine-based fuels. Although approximately 10^{18} different ionic liquids are possible [9], melting points are known for relatively few. The molecular design of new families of energetic ionic liquids would therefore be greatly aided by the derivation of quantitative structure-property relationships (QSPRs) for melting points of energetic ionic liquids.

Melting points for organic molecules depend on pairwise interactions and on the arrangement of atoms in the crystal lattice. Melting point prediction is hampered, in part, from the fact that these two properties are interdependent. Currently available descriptors were not designed for the description of condensed media [10]. However, additional factors that affect the strength of a crystal lattice and, therefore, the melting point, include molecular symmetry [11], the molecule's conformational degrees of freedom [11] and the molecular motion in crystals [12]. Both molecular symmetry and conformational degrees of freedom can be accounted for by descriptors obtained from gas-phase quantum mechanical calculations.

Strong electrostatic intermolecular forces typical of inorganic ionic compounds result in high melting points. Organic compounds have much weaker intermolecular forces, such as hydrogen bonding and dipole-dipole interactions. A melting point QSPR derived for 24 unbranched alkanes and composed entirely of topological indices is the

* The Anteon Corporation, 5100 Springfield Pike, Dayton, OH 45431-1231, steven.trohalaki@wpafb.af.mil

Supporting information for this article is available on the WWW under www.qsar-combsci.wiley-vch.de

 DOI: 10.1002/qsar.200430927

most accurate (RMS error = 0.5 °C) found for organic compounds [13]. However, the RMS error for the QSPR predicting the melting point of 56 alkanes, which also used connectivity indices, is much larger (23.8 °C) when normal and branched alkanes are considered [14]. In a study of 303 normal and branched substituted alkanes, an 11-term QSPR, whose descriptors characterize intermolecular forces, has an RMS error of 16.4 °C [15]. Katritzky, et al. [16], developed QSPRs for melting points of substituted benzenes and found that a hydrogen-bonding descriptor together with other quantum chemical descriptors led to correlations much improved over QSPRs derived with only topological, geometrical, and other traditional descriptors.

Because ionic liquids are weakly coordinating, accurate QSPRs for prediction of their melting point are expected to include descriptors that characterize weak intermolecular interactions. Melting point QSARs derived by Katritzky and coworkers for ionic liquids and ionic-liquid analogues [9, 17] are composed of information content indices [18] – descriptors characterizing the cations' size and electrostatics – and the average nucleophilic reaction index, i.e., the propensity of the cations to react with nucleophiles [19] The resulting melting point QSPRs have r^2 values ranging from 0.690 – 0.788, except for the QSPR derived for a subset of 18 substituted imidazolium bromides, which has an r^2 value of 0.943 [9, 17].

A new class of energetic ionic liquids, based on 1-substituted-4-amino-1,2,4-triazolium bromides, nitrates, and nitrocyanamides (see Figure 1), was recently synthesized and their melting points measured (see Table 1) [20]. The bromide salts number 13, the nitrate salts number 13, and the nitrocyanamides salts number 7. The range of melting points for the nitrates is about twice as that for the bromides. For a few of the salts in Table 1, the glass forms much more readily than the crystal and these data, therefore, actually correspond to glass transitions. In these cases, we employ glass transition temperatures in lieu of melting points because we want to predict the temperature at which the salt ceases to be a liquid. Drake et al. [20], reported that these new ionic liquids are stable at room temperature and show no signs of decomposition after more than a year at ambient temperatures. In general, the nitrate salts have lower melting points than the bromide salts. For the *n*-alkyl-substituted compounds, the melting points generally increase nonmonotonically with the length of the alkyl group. Compounds with an even number of substituent carbons generally display lower melting points that those with an odd number [20].

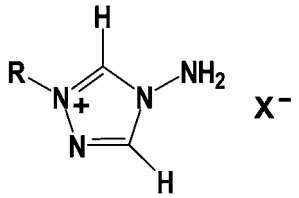

Figure 1. Molecular structure of ionic liquids based on 1-substituted-4-amino-1,2,4-triazolium. X^- is either Br^-, NO_3^-, or $NCNNO_2^-$ and R is a series of aliphatics or other common organic group (see Table 1).

We previously published melting point QSPRs for the bromide and nitrate salts using quantum descriptors calculated at the RHF/6-31G** level of theory [21]. Statistics for these QSPRs were good with r^2 values exceeding 0.9. We endeavor in this paper to derive improved melting point QSPRs for these new energetic ionic liquids by employing a higher level ab initio quantum method that accounts, in part, for electron correlation. In addition, we will derive for the first time melting point QSPRs for the nitrocyanamide salts. We will interpret these new QSPRs in terms of molecular interactions.

Table 1. Experimental and Calculated Melting Points of Ionic Liquids

Substituent	Bromide Salt			Nitrate Salt		Nitrocyanamide Salt	
	Exp.	Calc. Eq. 1	Calc. Eq. 2	Exp.	Calc. Eq. 3	Exp.	Calc. Eq. 4
methyl	92 °C	86.9 °C	88.4 °C	−54 °C (g)	−60.3 °C	11 °C	10.0 °C
ethyl	67	64.2	70.8	−55 (g)	−35.9	10	9.18
n-propyl	63	58.8	55.5	33	−2.6	5	6.00
isopropyl	92	93.1	97.6	66	63.8	–	–
2-propenyl	62	66.1	63.5	−50 (g)	−51.3	−11	−13.3
n-butyl	48	56.0	56.9	−50 (g)	−17.5	0	0.911
methylcyclopropyl	73	66.1	71.5	56	60.3	−10	−6.99
n-pentyl	54	53.9	57.4	29	30.7	–	–
n-hexyl	76	77.8	68.1	0	4.8	–	–
n-heptyl	94	85.1	89.1	35	46.4	–	–
n-octyl	80	86.2	83.7	34	31.0	–	–
n-nonyl	81	88.1	78.8	53	63.2	–	–
n-decyl	90	89.5	90.9	51	15.5	–	–
2-ethanol	–			–		0	−0.805

Data denoted with (g) correspond to glass transition temperatures, as explained in the text.

2 Methods

All *ab initio* quantum mechanical calculations were performed with Gaussian98, version A.9 [22]. Using the 6-31G** basis set (a split-valence basis set with polarization functions on all atoms), the optimal geometry for each cation (Table 1) was obtained using the restricted Hartree-Fock method (RHF) corrected for electron correlation using Møller-Plesset perturbation theory to second order (MP2) Although density functional theory (DFT) methods also account, in part for electron correlation but at about the same computational cost as HF (with the same basis set), a physical interpretation of unoccupied orbitals produced by DFT or HF-DFT hybrid methods is unclear [23] and utilization of descriptors that are functions of unoccupied orbitals is ill advised.

Using data supplied by Gaussian98 output files, CODESSA version 2.61 [24] was used to calculate all descriptors, although several descriptors like molecular orbital energies are simply extracted from the Gaussian98 output files. CODESSA was also employed to derive correlations between each descriptor and the melting point data, to derive the QSPRs, and to calculate the statistics for the QSPRs, including the correlation coefficient, r, the Fisher significance parameter, F, q, the cross-validated correlation coefficient calculated using a leave-one-out method, and the corrected mean square error, s. CODESSA's best multilinear regression method and heuristic method were used to obtain two-parameter and three-parameter melting point QSPRs. After screening out descriptors that are not defined for all compounds and that correlate poorly with the property data, the heuristic method was used to obtain one-parameter density QSPRs. Both methods limit the collinearity of the selected descriptors and utilize statistical significance to derive QSPRs.

CODESSA categorizes descriptors as constitutional, topological, geometrical, electrostatic, quantum mechanical, and thermodynamic, although both electrostatic and thermodynamic descriptors are obtained from quantum mechanics calculations. Constitutional, topological, geometrical descriptors were seldom found to be among the best descriptors and in only one case improved QSPRs that were derived without them. In this work, we therefore generally employed only electrostatic and quantum mechanical descriptors to derive QSPRs. The descriptor pool consisted of about 120 descriptors. Unless specified otherwise, the partial atomic charges that were employed were calculated using the Natural Bond Orbital method [25], as implemented in Gaussian98 [22].

3 Results and Discussion

Despite pertaining to the gas-phase, optimal molecular geometries of the cations compare well to the published crystal structures (the ethyl, *n*-propyl, *n*-hexyl, and *n*-heptyl bromide salts, were the only bromide salt crystal structures published [20] and the isopropyl and methylcyclopropyl nitrate salts which were the only two nitrate salt crystal structrures published) [20]. Calculated bonds lengths are in good agreement to those found in the crystal structures (see Supplementary Material). Although only bonds common to all cations are included in the Supplementary Material, experimental and theoretical bond lengths in the substituents are also in good agreement. A linear fit of a plot of calculated versus experimental bond lengths has an r^2 value of 0.972. The average RMS deviation for the bond lengths is 0.0162 Å. Calculated bond lengths reported here agree somewhat better with experiment than those we obtained previously using a lower level of quantum theory [21].

Good correlations with the experimental melting point data were found, although, for the bromide and nitrate salts, three parameters were required in order to obtain QSPRs with $r^2 > 0.8$. QSPRs derived for the melting points of the bromide salts are presented in Table 2a. The first QSPR in Table 2a displays good statistics but values of the third descriptor – the average valence of nitrogen atoms – differ only in the third decimal place (all descriptor values can be found in the Supplementary Material). Although this is certainly mathematically significant and the t-value for the third descriptor (see Table 2a) indicates that it is significant within the model, it is questionable whether such small differences in valences have real physical meaning. A plot of melting points calculated according to Equation 1 as a function of experimental values (see Figure 2) shows no outliers. Correlations between descriptors appearing in Eq. 1 are poor.

A melting-point QSPR with statistics superior to those for Eq. 1 can be obtained by employing topological and geometrical descriptors in addition to quantum mechanical descriptors. Eq. 2 (see Table 2a) employs descriptors from all 3 categories. In addition to somewhat better statistics, Eq. 2 may be preferable to Eq. 1 because all descriptors in Eq. 2 display wide ranges of values (see the Supplementary Material). However, topological descriptors are many times difficult to interpret in terms of physical mechanisms. As seen for Eq. 1, a plot of melting points calculated according to Eq. 2 as a function of experimental values (see Figure 3) shows no obvious outliers and correlations between descriptors appearing in Eq. 2 are poor. A QSPR derived for the melting points of the nitrate salts is presented in Table 2b. All 3 terms of Eq. 3 are quantum mechanical descriptors. Eq. 3 displays good statistics but, unlike the bromide salts, an improved QSPR does not result from inclusion of descriptors from other categories.

We found that a very good QSPR with a single descriptor – the occupied molecular orbital with the second highest energy (HOMO-1) – could be derived for the melting points of the nitrocyanamide salts if the propenyl compound was left out. Electron density plots showed that the HOMO-1 is located mostly on the substituents for all com-

Table 2a. Melting-Point QSPRs for Bromide Salts

Equation	r^2	q^2	F	s^2	Term	Coefficient	t-test	Descriptor
1	0.873	0.773	20.6	39.2	0	1.16×10^5 ($\pm 2.80 \times 10^4$)	4.15	Intercept
					1	-1.045×10^4 ($\pm 2.49 \times 10^3$)	−4.19	$NRI_{min,C}$: Minimum nucleophilic reactivity index for a carbon atom [19].
					2	-3.21×10^4($\pm 5.43 \times 10^3$)	−5.91	$ERI_{ave,C,subst}$: Average electrophilic reactivity index for carbon atoms comprising the substituent [19].
					3	-3.83×10^4 ($\pm 9.25 \times 10^3$)	−4.14	$V_{ave,N}$: Average valence of nitrogen atoms.
2	0.887	0.779	23.4	35.0	0	4.51×10^2($\pm 5.34 \times 10^1$)	8.43	Intercept
					1	-7.71×10^1(± 9.26)	−8.33	$IC_{ave,2}$: Average Information content (order 2) [30]
					2	-1.64×10^2($\pm 4.41 \times 10^1$)	−3.71	YZ Shadow / YZ Rectangle [31]
					3	-3.08×10^1(± 8.05)	−3.82	$WNSA2_{subst}$: Partial negative surface area weighted by the total charge and by the total molecular surface area. Calculated for the substituent [29].

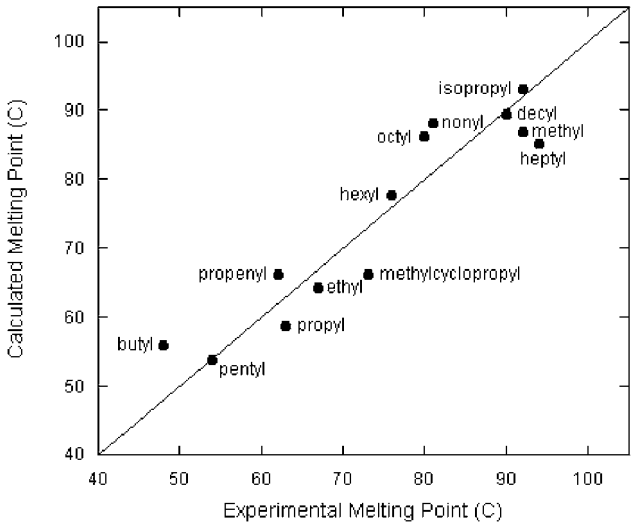

Figure 2. MPs calculated according to Eq. 1 are plotted as a function of experimental MPs. A line with a slope of unity was drawn to represent a perfect correlation between theory and experiment. See Table 2a for relevant statistics.

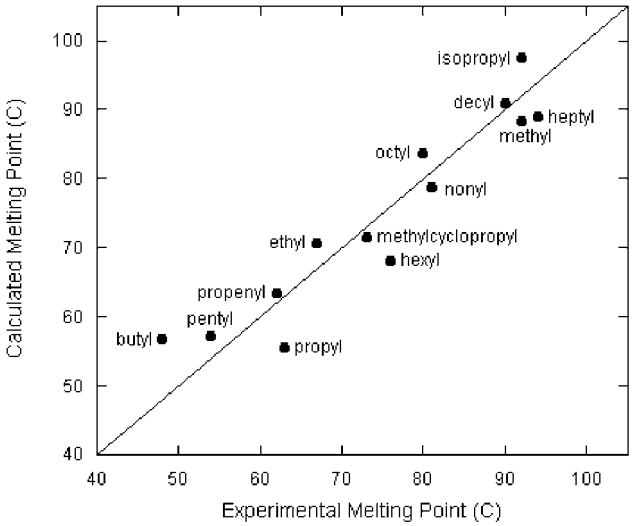

Figure 3. MPs calculated according to Eq. 2 are plotted as a function of experimental MPs. A line with a slope of unity was drawn to represent a perfect correlation between theory and experiment. See Table 2a for relevant statistics.

pounds except for the propenyl and 2-ethanol compounds. For these two compounds, the highest occupied molecular orbital (HOMO) is located on the substituents. We therefore defined a new descriptor – the highest occupied molecular orbital located on the substituent ($HOMO_{subst}$) – and derived an excellent one-parameter QSPR for the melting points of all 7 nitrocyanamide salts (see Table 2c). A plot of melting points calculated according to Equation 4 as a function of experimental values (see Figure 4) shows no outliers.

Reactvity indices [19], which are among the descriptors in Eqs. 1–3, are essentially Fukui functions [26] and are implicitly designed to describe chemical reactions. However, we infer that they serve here to quantify interactions between the cation and anion or between the cations themselves. Valence and charged surface areas, which also appear as descriptors in Eqs. 1–3, can be similarly interpreted. The sole shape descriptor (YZ Shadow/YZ Rectangle) in Eqs. 1–3 is intuitively credible as a melting-point descriptor because molecules need to pack in a crystal lattice. The $HOMO_{subst}$ descriptor in Eq. 4 can be interpreted in terms of frontier molecular orbital theory [27] (which describes the stabilization due to mixing of occupied MOs of one molecule with the unoccupied MOs of another) to describe interactions between the cation and the anion.

Topliss and Edwards [28] warn that multiple regression analyses utilizing a combination of a few compounds and a large pool of descriptors can result in chance correlations.

Table 2b. Melting-Point QSPR for Nitrate Salts

Eq	N	r^2	q^2	F	s^2	Term	Coefficient	t-test	Descriptor
3	13	0.839	0.721	15.6	475	0	3.80×10^3 ($\pm 5.96 \times 10^3$)	6.37	Intercept
						1	-2.01×10^5 ($\pm 3.24 \times 10^4$)	−6.21	$ERI_{ave,N}$: Average electrophilic reactivity index for nitrogen atoms [19].
						2	-6.03×10^4 ($\pm 1.10 \times 10^4$)	−5.51	$OERI_{max,C,subst,}$: Maximum one-electron reactivity index for carbon atoms in the substituent [19].
						3	$1.76e \times 10^2$ ($\pm 9.15 \times 10^1$)	1.92	$WNSA1_{NH2}$: Negatively charged solvent-accessible surface area of the amino moiety weighted by its total surface area [29].

Table 2c. Melting-Point QSPR for Nitrocyanamide Salts

Eq	N	r^2	q^2	F	s^2	Term	Coefficient	t-test	Descriptor
4	7	0.960	0.894	120	3.71	0	-1.12×10^2 ($\pm 1.03 \times 10^1$)	−10.9	Intercept
						1	−7.11 ($\pm$0.649)	−10.9	$HOMO_{subst}$: Highest occupied molecular orbital located on the substituent.

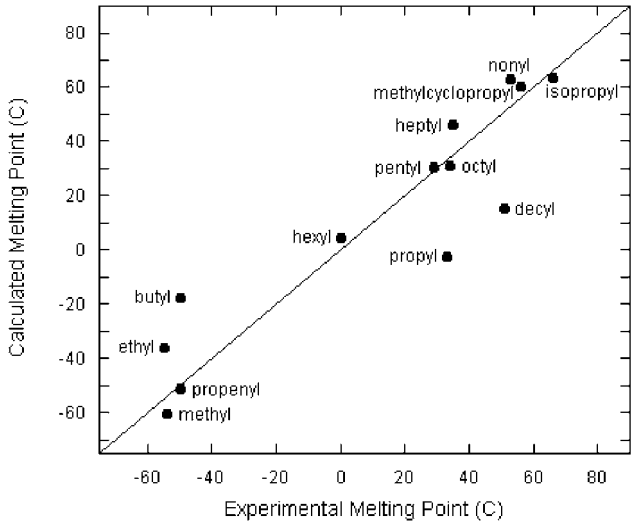

Figure 4. MPs calculated according to Eq. 3 are plotted as a function of experimental MPs. A line with a slope of unity was drawn to represent a perfect correlation between theory and experiment. See Table 2b for relevant statistics.

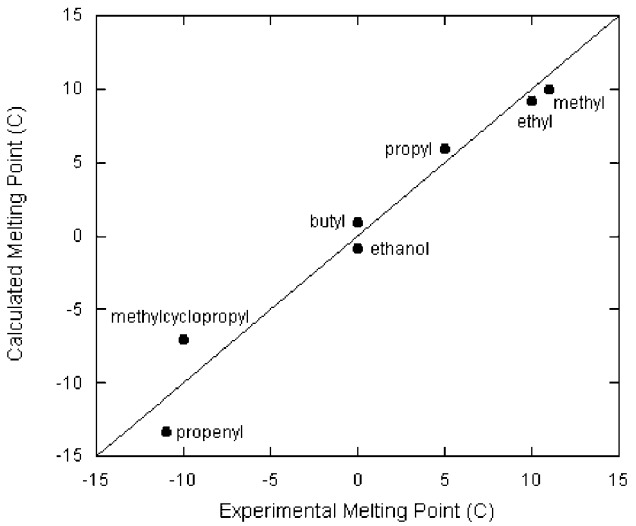

Figure 5. MPs calculated according to Eq. 4 are plotted as a function of experimental MPs. A line with a slope of unity was drawn to represent a perfect correlation between theory and experiment. See Table 2c for relevant statistics.

However, our pool of about 120 descriptors is reduced to fewer than 30 when ill-defined, insignificant, and intercorrelated descriptors are removed in the preliminary stages of CODESSA's best multilinear regression and heuristic methods. Furthermore, our reported t-values show that each parameter within each QSPR model is significant and our reported F-values are evidence that each QSPR model is significant.

The statistics for Eqs. 1–3 (see Tables 2a and 2b) are poorer than the statistics for the melting-point QSPRs we previously derived using quantum descriptors calculated at a lower level of ab initio theory [21]. For the bromide salts, we previously obtained a correlation with an r^2 value of 0.914 and a q^2 value of 0.784. For the nitrate salts, we previously obtained a correlation with an r^2 value of 0.933 and a q^2 value of 0.872 [21]. Our previous melting point QSPRs are composed of both reactivity indices and hydrogen-bond descriptors [29] but the latter are surprisingly lacking in the melting point QSPRs reported here.

4 Conclusions

We have presented QSPRs for the melting points of a new class of energetic ionic liquids that can be used in the design of additional 1-substituted-4-amino-1,2,4-triazolium bromide, nitrate and nitrocyanamide salts. Although several of the descriptors used here were originally intended to quantify chemical reactions, we believe that they serve here to describe the interactions between ions. Other descriptors, like charged surface areas, were intended to describe such interactions and serve that purpose here as well. Although acceptable, the statistics of the melting point QSPRs reported here are poorer than those for melting point QSPRs derived at a lower level of ab initio quantum theory, which we reported previously. Rather than resorting to higher levels of quantum theory, melting point QSPRs might be improved more substantially by designing descriptors specifically for ionic liquids.

Acknlowledgements

This work was funded by the US Air Force Office of Scientific Research. Calculations were performed with facilities provided by the Aeronautical Systems Center, Major Shared Resource Center at Wright-Patterson Air Force Base.

References

[1] T. Edwards, *J. Propul. Power* **2003**, *19*, 1089 – 1107
[2] W. C. Keller, *Aviat. Space Environ. Med.* **1988**, *59*, A100 – A106.
[3] S. Trohalaki, R. J. Zellmer, R. Pachter, S. M. Hussain; J. M. Frazier, *Toxicol. Sci.* **2002**, *68*, 498 – 507.
[4] T. Welton, *Chem. Rev.* **1999,** *99*, 2071 – 2083.
[5] P. Wasserscheid, W. Keim, *Agnew Chem. Int. Ed.* **2000**, *39*, 3772 – 3789.
[6] P. Wassersheid, T. Welton (Eds.), *Ionic Liquids in Synthesis*, Wiley-VCH, Weinheim, **2003.**
[7] R. Rogers, K. Seddon (Eds.) *Ionic Liquids Industrial Applications for Green Chemistry, ACS Symposium Series 818*. American Chemical Society: Washington, D.C., **2002.**
[8] J. S. Wilkes, *Green Chem.* **2002,** *4*, 3 – 10.
[9] A. R. Katritzky, R. Jain, A. Lomaka, R. Petrukhin, M. Karelson, A. E.Visser, R. D. Rogers, *J. Chem. Inf. Comput. Sci.* **2002**, *42*, 225 – 231.
[10] A. R. Katritzky, V. S. Lobanov, M. Karelson, *Chem. Soc. Rev.* **1995**, *24*, 279 – 287.
[11] J. C. Dearden, *Sci. Total Environ.* **1992**, *109*, 59 – 68.
[12] A. I. Kitiagorodsky, in: *Molecular Crystals and Molecules*, E. M. Loebl, (Ed.), Academic Press, New York, **1973.**
[13] M. P. Hanson, D. H. Rouvray, in: *Graph Theory and Topology in Chemistry*, R. B. King, D. H. Rouvray, (Eds.), Elsevier Science Publishers, Amsterdam, **1987**, *51*, 201 – 208.
[14] D. E. Needbam, I.-C.Wei, P. G. Seybold, *J. Am. Chem. Soc.* **1988**, *110*, 4186 – 4194.
[15] M. Charton, B.Charton, *J. Phys. Org. Chem.* **1994**, *7*, 196 – 206.
[16] A. R. Katritzky, U. Maran, M. Karelson, V. S. Lobanov, *J. Chem. Inf. Comput. Sci.* **1997**, *37*, 913 – 919.
[17] A. R. Katritzky, A. Lomaka, R. Petrukhin, R. Jain, M. Karelson, A. E. Visser, R. D. Rogers, *J. Chem. Inf. Comput. Sci.* **2002**, *42*, 71 – 74.
[18] L. B. Kier, *J. Pharm. Sci.* **1980**, *69*, 807 – 810.
[19] R. Franke, *Theoretical Drug Design Methods.* Elsevier, Amsterdam, 1984.
[20] G. Drake, T. Hawkins, K. Tollison, K. Hall, A. Vij, S. Sobaski, in: *ACS Sympsosium Series*, in press.
[21] S. Trohalaki, R. Pachter, G. Drake, T. Hawkins, *Energy & Fuels*, in press.
[22] Gaussian 98, Revision A.9, M. J. Frisch, G. W. Trucks, H. B. Schlegel, G. E. Scuseria, M. A. Robb, J. R. Cheeseman, J. A. Montgomery, Jr., T. Vreven, K. N. Kudin, J. C. Burant, J. M. Millam, S. S. Iyengar, J. Tomasi, V. Barone, B. Mennucci, M. Cossi, G. Scalmani, N. Rega, G. A. Petersson, H. Nakatsuji, M. Hada, M. Ehara, K. Toyota, R. Fukuda, J. Hasegawa, M. Ishida, T. Nakajima, Y. Honda, O. Kitao, H. Nakai, M. Klene, X. Li, J. E. Knox, H. P. Hratchian, J. B. Cross, C. Adamo, J. Jaramillo, R. Gomperts, R. E. Stratmann, O. Yazyev, A. J. Austin, R. Cammi, C. Pomelli, J. W. Ochterski, P. Y. Ayala, K. Morokuma, G. A. Voth, P. Salvador, J. J. Dannenberg, V. G. Zakrzewski, S. Dapprich, A. D. Daniels, M. C. Strain, O. Farkas, D. K. Malick, A. D. Rabuck, K. Raghavachari, J. B. Foresman, J. V. Ortiz, Q. Cui, A. G. Baboul, S. Clifford, J. Cioslowski, B. B. Stefanov, G. Liu, A. Liashenko, P. Piskorz, I. Komaromi, R. L. Martin, D. J. Fox, T. Keith, M. A. Al-Laham, C. Y. Peng, A. Nanayakkara, M. Challacombe, P. M. W. Gill, B. Johnson, W. Chen, M. W. Wong, C. Gonzalez, and J. A. Pople, Gaussian, Inc., Pittsburgh PA, 2003.
[23] R. Stowaser, R. Hoffman, *J. Am. Chem. Soc.* **1999**, *121*, 3414 – 3420.
[24] A. Katritzky, M. Karelson, V. S. Lobanov, R. Dennington; T. Keith, ©1994 – 1995
[25] NBO Version 3.1, E. D. Glendening, A. E. Reed, J. E. Carpenter, F. Weinhold.
[26] K. Fukui, *Theory of Orientation and Stereoselection*, Springer-Verlag, Berlin, **1975.**
[27] G. Klopman, R. F. Hudson, *Theoret. Chim. Acta* **1967**, *8*, 165 – 174.
[28] J. G. Topliss, R. P. Edwards, *J. Med. Chem.* **1979**, *22*, 1238 – 1244.
[29] D. T. Stanton, L. M. Egolf, P. C. Jurs, M. G. Hicks, *J. Chem. Inf. Comput. Sci.* **1992**, *32*, 306 – 316.
[30] L. B. Kier, *J. Pharm. Sci.*, **1980**, *69*, 807 – 810.
[31] R. H. Rohrbaugh, P. C. Jurs, *Anal. Chim. Acta*, **1987**, *199*, 99 – 109.

